Electrooptic Mapping of Near-Field Distributions in Integrated Microwave Circuits

Kyoung Yang, Gerhard David, *Member, IEEE,* Stephen V. Robertson, *Member, IEEE,* John F. Whitaker, *Member, IEEE,* and Linda P. B. Katehi, *Fellow, IEEE*

***Abstract*— A field mapping system based on external electrooptic sampling has been developed in order to determine the vectorial components of the electric near-field distribution within microwave integrated circuits. The capabilities of the setup are demonstrated by two-dimensional measurements of normal and tangential fields in a coplanar microwave distribution network at frequencies up to 15 GHz. Results obtained on a functioning power-distribution network, as well as on two nonfunctioning networks, show the ability of the technique to interrogate internal circuit operation and to isolate faults through investigation of the field distributions.**

***Index Terms*— Electric-field measurement, electrooptic measurements, integrated circuit testing, microwave measurements, nondestructive testing.**

I. Introduction

ELECTROMAGNETIC-FIELD probes are used for a variety of applications in RF metrology, where knowledge of electric-field structure is required. These include such diverse areas as the characterization of near-field patterns of antennas and antenna arrays, verification of electromagnetic compatibility (EMC) of electronic equipment, and failure diagnosis of microelectronic integrated circuits. Techniques using dipole- or monopole-type probes [1]–[3] have mainly been pursued, although the optically based technique of electrooptic sampling [4]–[5] has also been investigated. The features that make the electrooptic techniques very promising for near-field measurements are high bandwidth (into the terahertz regime for systems using ultrashort-pulse lasers as optical sources) and a spatial resolution on the order of the size of the laser-beam diameter or even less. Furthermore, electrooptic sampling does not require electrodes or ground planes as a part of the field probe so that, compared with conventional probes, the invasiveness is minimized.

Electrooptic measurements of field distributions of guided microwaves have been extensively demonstrated within monolithic microwave integrated circuits using the substrate of the circuits as the sensor element (internal electrooptic sampling). These measurements have revealed information for circuit characterization and failure detection [6]–[8] and could be used for verification of electromagnetic simulations. If the substrate does not exhibit the linear electrooptic effect and, moreover, when field patterns outside the substrate need to be known, external electrooptic sampling has to be used. This technique uses an electrooptic crystal as an electric-field probe, which is inserted into the electric field to be characterized. Measurements of near-field patterns of antennas and stray fields of simple waveguide structures [9]–[11] have been performed in this way. However, the potential of this technique with respect to the full characterization of the electric field inside integrated circuits, i.e., in terms of the different field components in amplitude and phase inside a microwave integrated circuit, has not been shown until now.

In this paper, measurements of near-field distributions of guided waves above an integrated microwave circuit are demonstrated using a distribution network having structure sizes down to 20 μm as an example device-under-test (DUT). The measurements are carried out using two different miniaturized probes. The footprints of these probes are reduced by a factor of 5–10 compared with conventional electrooptic probes that have been used, so that their size becomes equivalent to or even smaller than the investigated structures inside the DUT. The measurements reveal distinct field distributions of either the normal- or tangential-field components in amplitude and phase. Using this information, the performance of circuit elements has been analyzed up to 20 GHz thus far. Moreover, fault isolation has been performed, comparing results obtained in a functioning structure operated accordingly to its design and several nonfunctioning structures. This has demonstrated the ability of this mapping technique to locate malfunctioning devices by studying the electric-field distribution of a circuit.

II. Measurement System Configuration

The measurement setup used is shown in Fig. 1. The optical beam from a phase-stabilized Ti:sapphire laser (pulse length: 80 fs, repetition rate: 80 MHz) is focused inside the electrooptic probe crystal. The incident beam is totally reflected, so that no illumination of the circuit-under-test occurs. The reflected beam is analyzed with respect to the change of the polarization state, which is sensitive to the circuit electric field reaching the probe. This is performed using a Pockels-cell arrangement consisting of a combination

Manuscript received March 27, 1998; revised August 3, 1998. This work was supported by the MURI on "Spatial and Quasi-Optic Power Combining" monitored by the Army Research Office Grant DAAG-55-97-0132 under subcontract to Clemson University, and by the National Science Foundation through the Center for Ultrafast Optical Science under Contract STC PHY 8920108. The work of G. David was supported by a Feodor–Lynen Fellowship of the Alexander von Humboldt Foundation, Germany.

K. Yang, G. David, J. F. Whitaker, and L. P. B. Katehi are with the Center for Ultrafast Optical Science and Radiation Laboratory, Department of Electrical Engineering and Computer Science, University of Michigan at Ann Arbor, Ann Arbor, MI 48109-2122 USA.

S. V. Robertson is with the Wireless Technology Laboratory, Lucent Technologies, Whippany, NJ 07981-0903 USA.

Publisher Item Identifier S 0018-9480(98)09199-6.

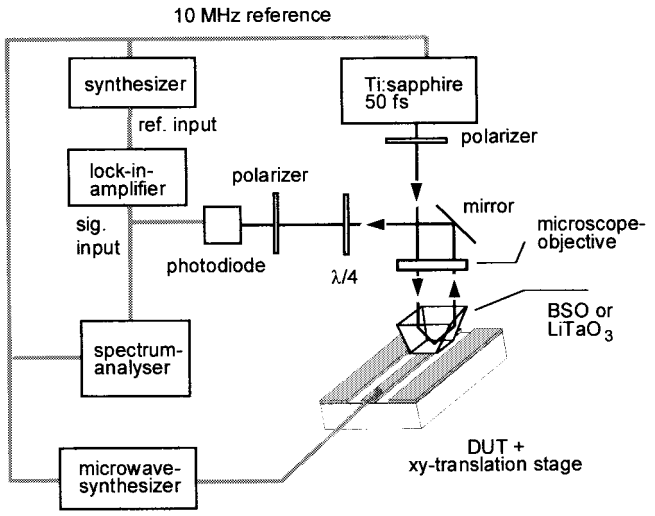

Fig. 1. Electrooptic-probe station schematic.

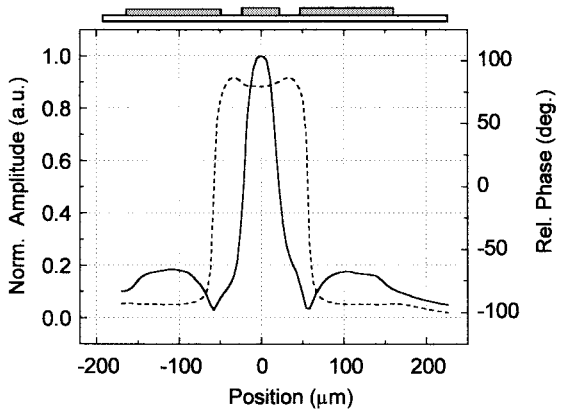

Fig. 2. Electrooptic mapping of the normal-field component of the even mode on a CPW (transverse direction) measured using BSO, $f = 5$ GHz, solid line: normalized amplitude, dashed line: phase (the center conductor has a width of 40 μm, with spacings of 24 μm).

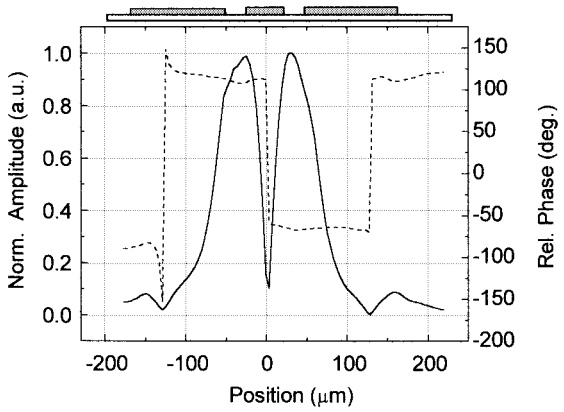

Fig. 3. Electrooptic mapping of tangential-field component in the x-direction of the even mode on a CPW (transverse direction) measured using $LiTaO_3$, $f = 15$ GHz, solid line: normalized amplitude, dashed line: phase.

of polarizers and retardation plates. The electrooptic signal is measured in a harmonic mixing scheme [4] at an intermediate frequency of several megahertz using an RF lock-in amplifier or a spectrum analyzer. Due to phase-locked loop electronics in the laser system, it is possible to synchronize continuous wave (CW) signals from a microwave synthesizer to the laser pulse train so that measurements in amplitude and phase can be performed.

The two types of electrooptic probes employed in this paper were fabricated from Bismuth Silicate (BSO) and Lithium Tantalate ($LiTaO_3$), which allow the determination of the normal- and tangential-field components, respectively. The crystals have a footprint of 40 $\times$ 40 μm for the BSO, and 20 $\times$ 10 μm for the $LiTaO_3$. Additionally, high spatial resolution is obtained by focusing the laser beam to a small spot at the bottom of the probe. The distance between probe and DUT is adjusted to be 5–7 μm. This distance avoids capacitive loading of the circuit and, therefore, minimizes the invasiveness of the measurement technique [12]. The minimum detectable voltage is measured to be about 1 mV or -45 dBm for 50-Ω geometries, and the sensitivity is 40 mV/$\sqrt{\text{Hz}}$. The DUT is mounted on a computer-controlled x–y translation stage, and the microwave signal is applied via on-wafer probes. Typical measurements including 6400 points are carried out in approximately 45 min. This duration is mainly limited by the speed of the translation stage and, therefore, can be improved substantially in the future.

III. Experimental Results

A. Coplanar Waveguide (CPW)

Figs. 2 and 3 display typical electrooptic-field maps of the electric normal- and tangential-field components for an even mode on a CPW in the transverse direction. Fig. 2 shows one-dimensional (1-D) mapping at 5 GHz using BSO, with a high electrooptic signal on the center conductor and a low electrooptic signal on the ground conductor corresponding to the strength of the normal field component. A phase change of 180° between the center conductor and two ground planes is observed. Fig. 3 shows 1-D measurements of the tangential components at 15 GHz using the $LiTaO_3$ probe. Corresponding to the strength of the tangential-field component in the x-direction (for coordinate system, see Fig. 1), the maximum signal appears above the spacings with a phase change of 180° taking place over the center conductor. These 1-D-field maps demonstrate the excellent discrimination in electric-field components available using external electrooptic sampling.

B. Microwave Distribution Network

The examined distribution-network circuit is a coplanar design (see Fig. 4) fabricated on high-resistivity Si. It is based on two Wilkinson power dividers, which distribute the input microwave signal to four output ports. The ports are terminated with 50-Ω thin film resistors, and this matched circuit is considered to be the correctly functioning circuit. The small lines crossing the coplanar structure at discontinuity points are air bridges, and impedance transformations appear at several places.

Two malfunctioning circuits of the same type were also examined. In the first circuit, the termination resistors are missing so that the output ports are open terminated. The

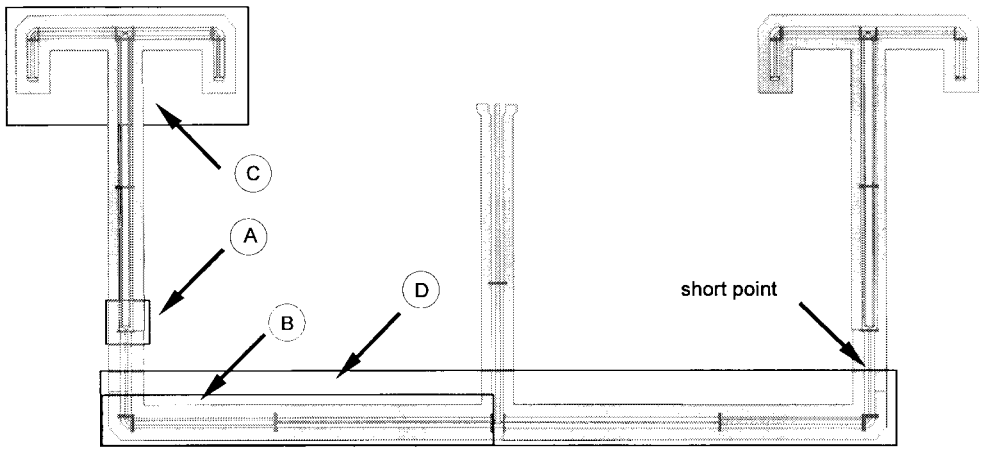

Fig. 4. Distribution-network circuit with investigated areas, chip size: 8.3 mm × 3.7 mm.

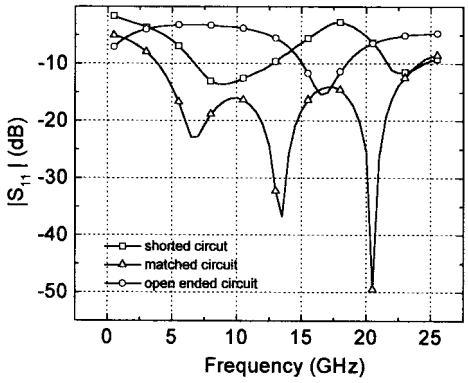

Fig. 5. Magnitude of the forward reflection coefficient $|S_{11}|$ for the examined distributions networks.

second circuit is fabricated with a short between the center and one ground conductor near the upper side output of one CPW bend, as indicated in Fig. 4.

Fig. 5 shows the results of one port s-parameter measurements of the examined circuits using a conventional microwave network analyzer (HP 8510B). The three curves represent the forward reflection coefficients of the matched, partially shorted, and open-ended circuit, respectively. The matched circuit shows very low reflection in comparison with the two other circuits, revealing its functionality as a distribution network. These measurements clearly show the malfunction of the shorted and open-ended circuit, but they cannot deliver information about the concrete location of the faulty components inside the circuits.

In the rest of this section, examples of two-dimensional (2-D) field distributions inside the circuits measured using the electrooptic probe station are presented. These measurements reveal additional information about the functioning and malfunctioning performance of the circuits which is not accessible using the external port s-parameter measurement technique.

As an example of the vectorial measurement capabilities of the electrooptic technique, Fig. 6 displays the normal- and tangential-field distribution around the input of the Wilkinson power divider (position A in Fig. 4). Fig. 6(a) and (b) shows field distributions that are in good agreement with the 1-D-field maps in Figs. 2 and 3 that have already displayed transverse distributions of the even mode. That is, we can see how the high normal fields are present above the center conductors of the CPW's for the normal-field probe, and how the tangential-field probe senses a high signal in the spacings of the waveguide. Additionally, the 2-D measurements now reveal that a small asymmetric coupling into both signal lines of the Wilkinson divider occurs. From Fig. 6(c) and (d), it can also be concluded that, at this frequency, no significant coupling between the lines is present, since only small tangential-field components can be measured in the spacing between them. Note also in all figures that the air bridges screen the electric field of the underlying waveguide from the probe.

Fig. 7 shows measurements in position B of the network where the length of the transmission line is comparable with the wavelength for the 15-GHz input signal. Fig. 7(a) and (b) displays the result for the functioning circuit and reveal a propagating microwave signal. The phase along the center conductor is changing 140°, which is in good agreement with the expected wavelength of 7.9 mm of the 15-GHz microwave signal on the transmission line. The field amplitude is also consistent across the length of the line, although an impedance transformation from 70 to 50 Ω in the middle of the line changes the CPW dimensions and, thus, also the field strength that the probe is sensing on either side of the discontinuity. In contrast to this result, the field distribution in the same area for the structure with the open termination at its four outputs reveals a standing-wave pattern [see Fig. 7(c) and (d)]. Field minima and maxima are observed in the amplitude of the open-circuit pattern with a phase shift of 180° between the maxima.

Fig. 8 shows the 2-D normal-field distribution of the output of the Wilkinson power divider feeding the two output ports (position C in Fig. 4). Fig. 8(a) again displays a propagating microwave signal with uniform field amplitude on the individual divider elements, while this effect cannot be seen in Fig. 8(b). Here, the effect of a standing wave with maxima at the terminations is observed, indicating a mismatch of the termination thin-film resistors. For Fig. 8(a), the electrooptic signals from the vertical and horizontal parts of the structure

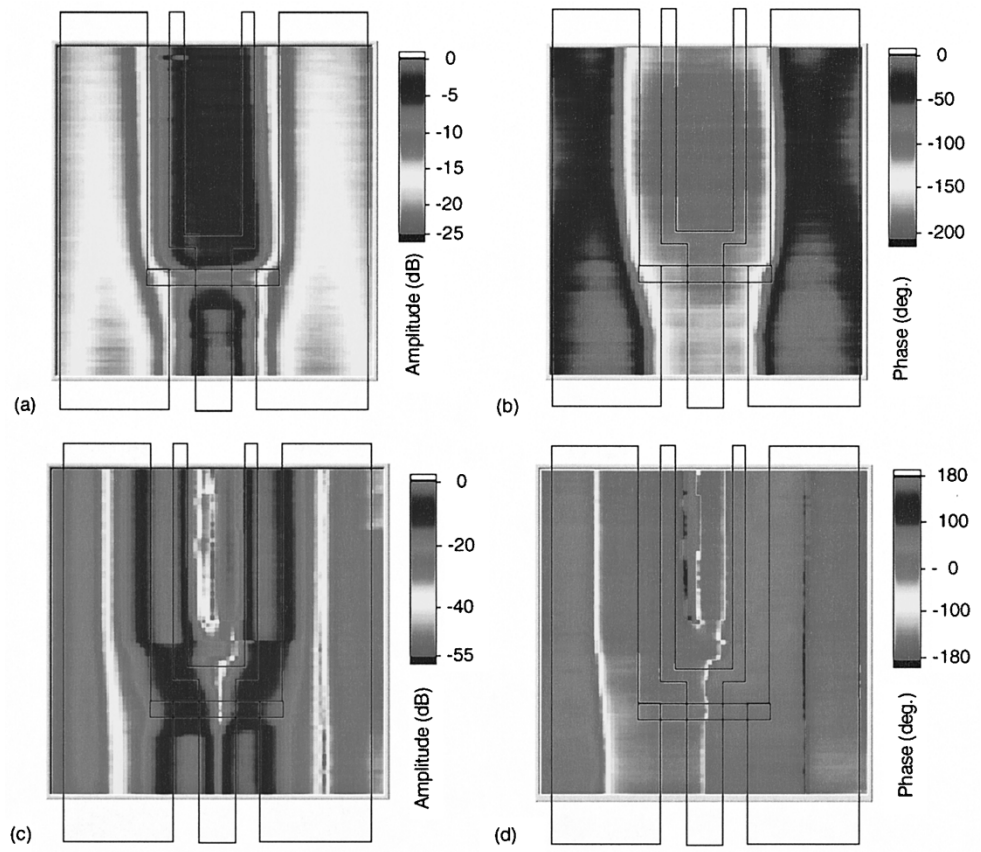

Fig. 6. Electrooptic-field mapping at the input of the Wilkinson power divider at position A in Fig. 4, $f = 15$ GHz [scanned area: 375 μm $\times$ 400 μm for (a) and (b) and 400 μm $\times$ 400 μm for (c) and (d)]. (a) Normalized amplitude of normal component in decibels. (b) Relative phase of the normal component in degrees. (c) Normalized amplitude of tangential component in decibels. (d) Relative phase of the tangential component in degrees.

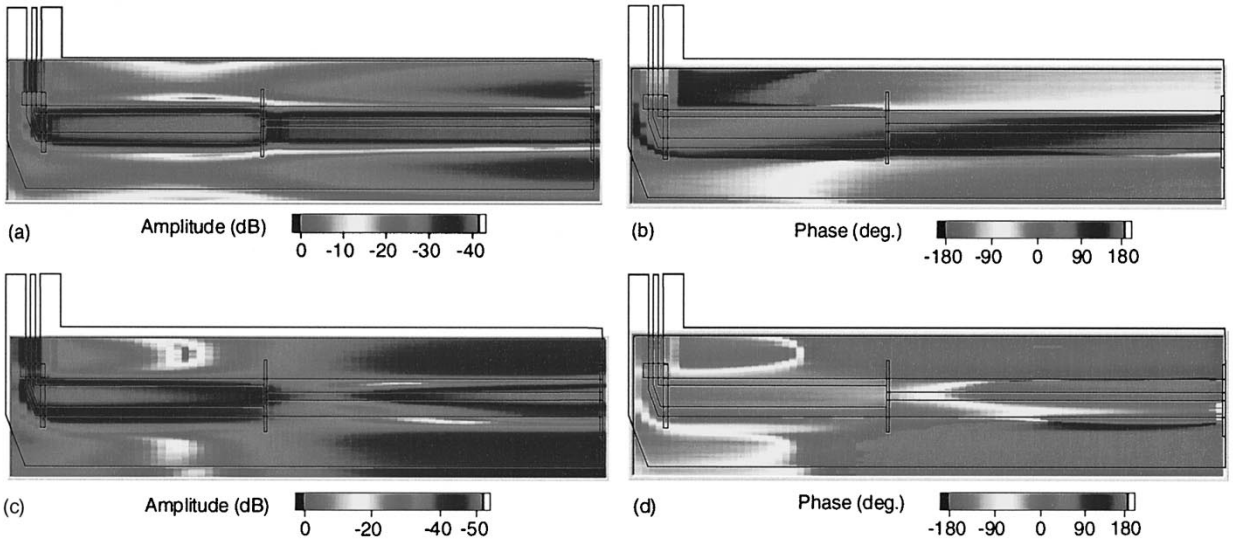

Fig. 7. Electrooptic-field mapping of the transmission line at position B in Fig. 4, $f = 15$ GHz, scanned area: 3400 μm $\times$ 400 μm. (a) Normalized amplitude of normal component in decibels (functioning circuit). (b) Relative phase of the normal component in degrees (matched circuit). (c) Normalized amplitude of normal component in decibels (open-ended circuit). (d) Relative phase of the normal component in degrees (open-ended circuit).

are not the same because, as for the impedance transformer, different line dimensions yield different field strengths.

Fig. 9 shows 2-D measurements of the normal-field components in position D of the matched and shorted circuit. The short point is intentionally fabricated approximately 200 μm above the upper output of one of the CPW bends (position marked in Fig. 4). The matched circuit shows a symmetric field distribution along the transmission lines [see Fig. 9(a)], revealing a propagating microwave signal, as well as equal field strengths along the right-hand- and left-hand-side vertical

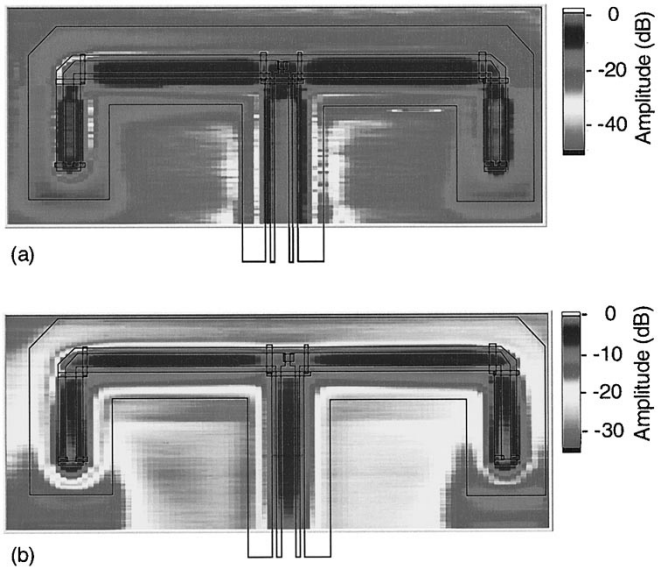

Fig. 8. Electrooptic mapping of the normal-field component of the output of the Wilkinson divider including termination at position D in Fig. 4, $f = 15$ GHz, scanned area: 3200 μm $\times$ 940 μm). (a) Normalized amplitude in decibels (matched circuit). (b) Normalized amplitude in decibels (open-ended circuit).

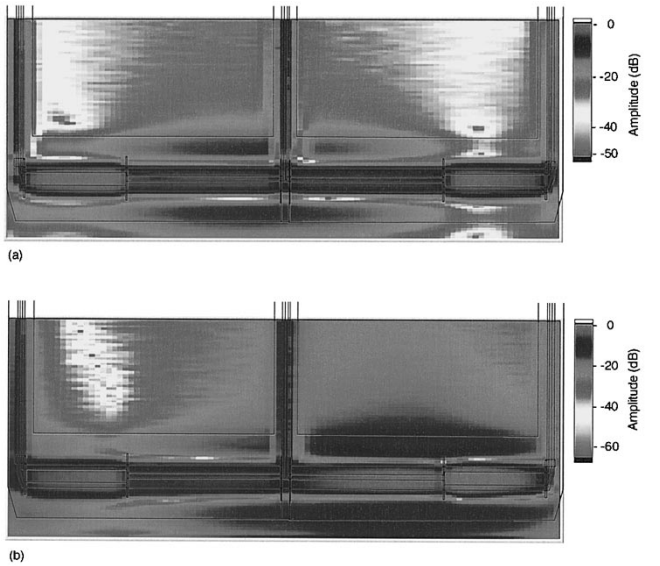

Fig. 9. Electrooptic-field mapping of the transmission line at position C in Fig. 4, $f = 15$ GHz, normalized amplitude of normal component in decibels. (a) Matched circuit. (b) Partially shorted circuit.

lines. In contrast, the shorted circuit shows an asymmetric distribution, with a complete absence of normal electric field on the right-hand-side vertical structure. As can be seen from Fig. 9(b) in the amplitude, and additionally from the corresponding phase measurement (not shown here), a standing-wave pattern is present in front of the short point, while the microwave signal cannot be detected passing the short point.

IV. Conclusions

2-D near-field mapping of a microwave-distribution network is performed, revealing insight into the normal- and tangential-field components inside the circuit. The technique makes it possible to investigate the microwave performance of single components within a circuit. An analysis of effects due to electrical short and open termination of the output ports has provided information on how such faults affect the internal operation of the circuit. In conclusion, the results demonstrated that the external electrooptic-field mapping technique is a powerful tool for a wide range of applications in RF near-field characterization.

References

[1] A. D. Yaghijian, "An overview of near-field antenna measurements," *IEEE Trans. Antenna Propagat.*, vol. AP-34, pp. 30–45, Jan. 1986.
[2] T. Budka, S. D. Waclawik, and G. Rebeiz, "A coaxial 0.5–18-GHz near electric field measurement system for planar microwave circuits using integrated probes," *IEEE Trans. Microwave Theory Tech.*, vol. 44, pp. 2174–2183, Dec. 1996.
[3] Y. Gao and I. Wolff, "A new miniature magnetic field probe for measuring three-dimensional fields in planar high frequency circuits," *IEEE Trans. Microwave Theory Tech.*, vol. 44, pp. 911–918, Dec. 1996.
[4] B. H. Kolner and D. M. Bloom, "Electrooptic sampling in GaAs integrated circuits," *IEEE J. Quantum Electron.*, vol. QE-22, pp. 79–93, Jan. 1986.
[5] J. Valdmanis and G. Mourou, "Subpicosecond electrooptic sampling: Principles and applications," *IEEE J. Quantum Electron.*, vol. QE-22, pp. 69–78, Jan. 1986.
[6] M. G. Li, E. A. Chauchard, C. H. Lee, and H.-L. A. Hung, "Two-dimensional field mapping of GaAs microstrip circuit by electrooptic sensing," in *OSA Proc. Picosecond Electron. and Optoelectron.*, Salt Lake City, UT, Mar. 1991, pp. 54–58.
[7] G. David, S. Redlich, W. Mertin, R. M. Bertenburg, S. Koßlowski, F. J. Tegude, and D. Jäger, "Two-dimensional direct electro-optic field mapping in a monolithic integrated GaAs amplifier," in *Proc. 23rd EuMC*, Madrid, Spain, Sept. 1993, pp. 497–499.
[8] G. David, R. Tempel, I. Wolff, and D. Jäger, "Analysis of microwave propagation effects using 2-D electro-optic field mapping techniques," *Opt. Quantum Electron.*, vol. 28, pp. 919–931, July 1996.
[9] K. Kamogawa, I. Toyoda, K. Nishikawa, and T. Tokumitsu, "Characterization of a monolithic slot antenna using an electrooptic sampling technique," *IEEE Microwave Guided Wave Lett.*, vol. 4, pp. 414–416, Dec. 1994.
[10] T. Pfeifer, H.-M. Heiliger, T. Loeffler, C. Ohlhoff, C. Meyer, G. Luepke, G. Roskos, and H. Kurz, "Optoelectronic on-chip characterization of ultrafast electric devices: Measurement techniques and applications," *IEEE J. Select Topics Quantum Electron.*, vol. 2, pp. 586–604, Sept. 1996.
[11] T. Pfeifer, T. Loeffler, H. G. Roskos, H. Kurz, M. Singer, and E. M. Biebl, "Electrooptic near-field mapping of planar resonators," *IEEE Trans. Antenna Propagat.*, vol. 46, pp. 284–291, Feb. 1998.
[12] T. Nagatsuma, T. Shibata, E. Sano, and A. Iwata, "Subpicosecond sampling using a noncontact electro-optic probe," *J. Appl. Phys.*, vol. 66, pp. 4001–4009, Nov. 1989.

Kyoung Yang was born in Seoul, Korea, in 1968. He received the B.S. and M.S. degrees in electrical engineering from Seoul National University, Seoul, Korea, in 1990 and 1993, respectively, and is currently working toward the Ph.D. degree in electrical engineering and computer science at the University of Michigan at Ann Arbor.

His current research interests include the development of high-speed electrooptic and photoconductive measurement techniques for the characterization of microwave and millimeter-wave circuits and radiators.

Gerhard David (M'97), for photograph and biography, see this issue, p. 2336.

Stephen V. Robertson (M'92) received the B.S.E.E. degree from the University of Texas at Austin, in 1991, and the M.S.E. and Ph.D. degrees from the University of Michigan at Ann Arbor, in 1993 and 1997, respectively.

While at the University of Michigan at Ann Arbor, he was a Member of the Radiation Laboratory, where his research efforts focused on the development of silicon micromachining technology for microwave and millimeter-wave circuits. In 1998, he joined the Wireless Technology Laboratory, Lucent Technologies, Whippany, NJ.

John F. Whitaker (S'84–M'88), for photograph and biography, see this issue, p. 2336.

Linda P. B. Katehi (S'81–M'84–SM'89–F'95) received the B.S.E.E. degree from the National Technical University of Athens, Athens, Greece, in 1977, and the M.S.E.E. and Ph.D. degrees from the University of California at Los Angeles, in 1981 and 1984, respectively.

In September 1984, she joined the faculty of the Electrical Engineering and Computer Science Department, University of Michigan at Ann Arbor. Since then, she has been interested in the development and characterization (theoretical and experimental) of microwave, millimeter printed circuits, the computer-aided design of very large-scale integration (VLSI) interconnects, the development and characterization of micromachined circuits for millimeter-wave and submillimeter-wave applications, and the development of low-loss lines for terahertz-frequency applications. She has also been theoretically and experimentally studying various types of uniplanar radiating structures for hybrid-monolithic and monolithic oscillator and mixer designs.

Dr. Katehi is a member of IEEE AP-S, MTT-S, Sigma Xi, Hybrid Microelectronics, URSI Commission D and a member of AP-S ADCOM (1992–1995). She is an associate editor for the IEEE TRANSACTIONS OF THE MICROWAVE THEORY AND TECHNIQUES. She was awarded the IEEE AP-S R. W. P. King Best Paper Award for a Young Engineer in 1984, the IEEE AP-S S. A. Schelkunoff Best Paper Award in 1985, the NSF Presidential Young Investigator Award and URSI Young Scientist Fellowship in 1987, the Humboldt Research Award and The University of Michigan Faculty Recognition Award in 1994, the IEEE MTT-S Microwave Prize in 1996, and the 1997 Best Paper Award from the International Microelectronics and Packaging.